Modeling and Sustainability Assessment of Outdoor *Chlorella vulgaris* Cultivation in South Korea for Renewable Bioplastic Feedstock Production

Jeehwan Lee*, Seongmin Heo, Jay H. Lee***

**Department of Chemical and Biomolecular Engineering, Korea Advanced Institute of Science and Technology (KAIST), Boulder, 291 Daehak-ro, Yuseong-gu, Daejeon 34141, Republic of Korea (Tel: 042-350-3966; e-mail: stevelee@kaist.ac.kr, jayhlee@kaist.ac.kr).*

***Department of Chemical Engineering, Dankook University, Yongin 16890, Republic of Korea (e-mail: smheo@dankook.ac.kr)*

Abstract: UTEX 2714 (*Chlorella vulgaris*) is cultivated outdoors in vertical bubble columns contained within a greenhouse to serve as a renewable blending bioplastic feedstock (BPFS). This application has potential advantages over traditional biofuels due to a simpler downstream process and higher marketability of the bioplastic product (> 1200 USD/ton). To assess sustainability for further scale-up and predict growth for varying seasonal conditions, mathematical modeling of growth kinetics was performed. Pilot plant data for parameter estimations were provided by the Pangyo LNG power plant complex. For early June 2021 during which the data was collected, algae productivity was 0.13 kg/m^3/day, with the unit cost of production and specific carbon footprint being 2768 USD/ton and 1.33 ton CO_2-eq/ton, respectively. Monthly average productivity dipped to 0.061 kg/m^3/day in February and peaked at 0.16 kg/m^3/day in early August. Seasonal variations in temperature and light intensity significantly influenced the economic viability and greenhouse gas emission reducibility of the BPFS process, which highlights the need to improve the accuracy of the growth prediction model and expand the risk assessment scope for guiding future R&D.

Keywords: Algae growth modeling, Outdoor cultivation, Growth kinetics, Bioplastic feedstock, Biological CCU

1. INTRODUCTION

Microalgae is considered as a platform for biological carbon capture and utilization (CCU) due to its ability to autotrophically bio-fix CO_2. It has especially garnered interest as a renewable feedstock for biofuels due to its high areal lipid productivity of >90,000 L/hectare (Demirbas and Fatih Demirbas, 2011). A major criticism of microalgae for biofuels applications, however, is the costly and complicated downstream that is required to produced the end fuel. Biodiesel, for example, can only be derived from cell lipids, which first requires penetration of the cell wall and extraction before any conversion can occur. For virtually all biofuel applications, large amounts of water need to be removed to concentrate the biomass. These harvesting, dewatering and drying steps can be highly energy-intensive, leading to low energy efficiencies (Razon and Tan, 2011). The combination of low lipid yields, high processing costs and energy demands means that the sustainability of microalgae-to-biofuel technologies is uncertain. On the other hand, production of highly valorisable products such as dietary supplements (*e.g.* astaxanthin) are restricted to small, niche markets (Li et al., 2020), which limits the ability to effectively reduce greenhouse gas (GHG) emissions on a large scale.

In this regard, microalgae as a bioplastic feedstock (BPFS) can be a viable alternative. Algal biomass is co-blended with traditional polymers to create a bioplastic resin that has both improved biodegradability and lower carbon footprint of production than conventional polymers (Zeller et al., 2013). The feasibility of algae-plastic blending has been demonstrated in previous works such as M. Crocker et al. (2020) in which freshwater UTEX B72 was blended with ethylene vinyl acetate (EVA) (Crocker et al., 2020). For biomass-EVA blends, the minimum selling price ranges between 1500 – 2000 USD/ton, compared to biofuels at 800 – 1300 USD (Gerber et al., 2016). Moreover, preparation of BPFS requires minimal downstream processing. After drying, the entirety of the biomass with <10 wt% moisture can be blended, although additional treatment steps such as lipid extraction, and biomass fractionation can further improve bioplastic properties (Crocker et al., 2018).

In this work, we consider BPFS preparation via drying only, in which further heat integration is achieved by rerouting stack flue gases to the convective dryer. Despite these process improvements, the economic feasibility and environmental sustainability of algal BPFS production is still dubious and highly dependent on natural variabilities. Temperature and sunlight intensity, in particular, directly influence the growth rate of the biomass (Béchet et al., 2013), which affects both efficiency and productivity. Meanwhile, cultivation experiments are known to be time consuming. A single batch growth experiment can take multiple days and requires many intermediate measurements. In order to estimate and assess the sustainability of the BPFS process under varying natural conditions, mathematical modeling of cell growth and key downstream units was conducted. Unit cost of goods manufactured (COGM, USD/ton BPFS) and specific carbon footprint (ton CO_2-eq/ton BPFS) were measured as

performance indicators for economic and environmental sustainability, respectively.

2. CULTIVATION PILOT PLANT

2.1 Plant specifications

UTEX 2714 (*Chlorella vulgaris*) was cultivated in a 15 m^3 pilot plant. The plant was constructed on-site at the Pangyo LNG-fired power facility in South Korea and consists of a greenhouse encompassing an area of 50m^2 with fifteen photobioreactor (PBR) modules. Each PBR module has a culture volume of 1 m^3 that is contained within LDPE airlift bags and supported on a stainless steel superstructure (Fig. 1). The LDPE bags are arranged horizontally in a design similar to the Green Wall Panel®-II and have a maximum thickness of 20 cm, approximate height of 1.2m and a length of 4.2m.

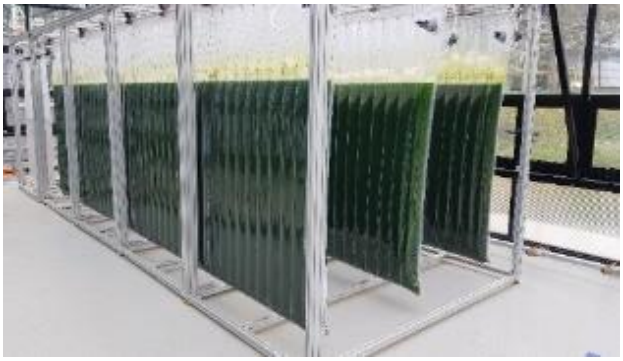

Figure 1. Stainless steel supported vertical airlift PBRs inside a greenhouse at the Pangyo facility. Each row contains a culture volume of 1m^3.

The 1m^3 PBR module each occupies 3.3m^2 of land and requires 3 kg of LDPE, which are replaced every two years. CO_2 is supplied via flue gas aeration from the power plant stack, which also provides vertical mixing. Flue gas is supplied to the PBR system as a bypass, meaning that any lean gases and PBR off-gases are rerouted to the stack. The composition of CO_2 in the flue gas ranges between 4 – 6 vol%. For the purpose of establishing mass balances, the values reported in Scholes et al. were used (Scholes et al., 2016) (Table 1).

Table 1. Temperature and composition of LNG-fired flue gas as reported in Scholes et al.

Temperature (°C)	100°C
Composition (mol %)	
CO_2	4.97
N_2	74.28
O_2	9.73
H_2O	11.02

2.2 Data collection and processing

The experimental data for growth parameter estimation was conducted over a 149 hour period between June 2nd to June 9th 2021. Cell concentration (g/L), light intensity (µE/m^2s), and temperature (°C) were measured at roughly 90 second intervals. The target cell concentration for biomass harvesting was set to 1 g/L.

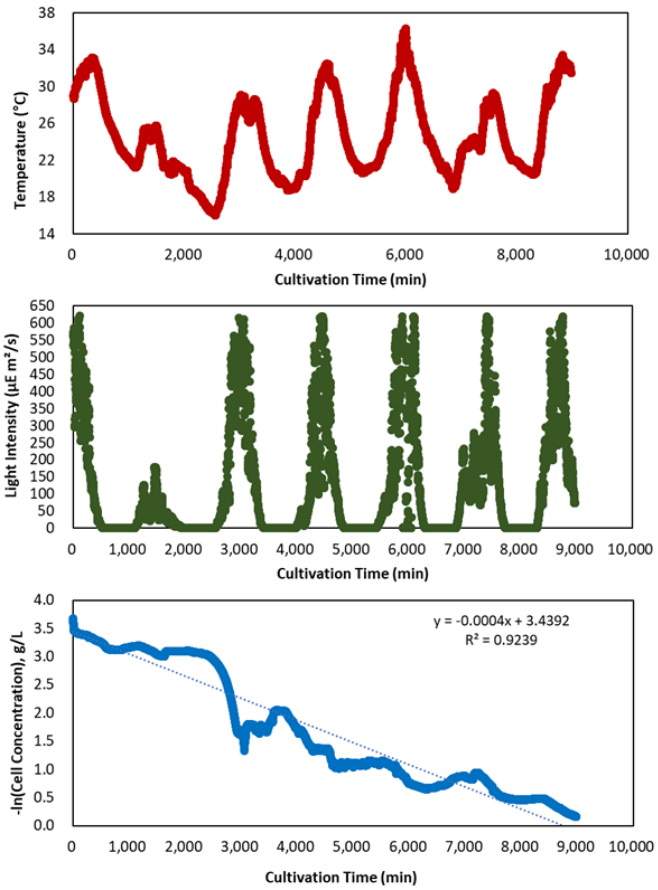

Figure 2. Experimental data for culture temperature, light intensity inside the greenhouse and cell concentration.

Due to outdoor cultivation, the collected data was noisy, particularly with respect to light intensity. It was observed that the recorded light intensity would spontaneously fall to 0 during the daylight hours. The cause was later determined to be shadows that were cast from the steel superstructure covering the light sensors, for which it instantaneously read very low intensities. The data for light intensity and temperature were post-processed with ARIMA for outlier removal. ARIMA(2,0,1) was fitted, corresponding to 2 autoregressive time lags and 1 moving average time lags. The dynamic threshold was set to *mean(error) + 3·stdev(error*).

3. CELL GROWTH MODELING

3.1 Characterizing cell growth and death

A plot of the log of cell concentration versus time showed approximate first order kinetics with an R^2 error of 0.92. Periods of cell concentration decrease during the night was observed, with particularly significant death occurring in night 4. We postulate multiple reasons for night-induced death, including programmed cell death (PCD), low temperature due to absence of light, and a decrease in culture pH. The latter can occur because flue gas is still being supplied during the night, albeit at a lower flowrate of 0.02 v.v.m., in order to provide aeration and prevent settling. Due to the absence of photosynthesis, carbonic acid can build up in the culture. However, low pH alone does not describe why significant cell death was observed only on night 4.

Following first order kinetics, cell concentration can be represented via the following equation

$$C_x(t) = C_{x0}e^{\mu_g - \mu_D} \quad (1)$$

μ_g and μ_d represent rate constants for cell growth and cell death, respectively. In the current PBR system, growth nutrients were present in excess in the culture media and CO_2 was continuously supplied during the daylight hours at 0.05 v.v.m. Consequently, μ_g and μ_d were modeled as functions of light intensity and culture temperature. Various forms of rate expressions for light/temperature-limited growth have been proposed in literature and can be broadly classified into either threshold or multiplicative models (Lee et al., 2015). Threshold models are based on the minimum law and models growth rate based on the most limiting condition. In the threshold model proposed by Guest et al. for example, co-limitation of light intensity and N, P nutrients was considered (Guest et al., 2013). Multiplicative models, on the other hand, assume that relevant growth conditions influence growth equally and simultaneously. Each contributing factor is represented as a multiplicative term in the rate expression.

3.2 Modeling growth rate

For the growth rate μ_g, a screening of existing multiplicative models that consider light intensity (I) and temperature (T) was performed. The model proposed by Franz et al. (2) was ultimately selected on the basis of best fit and lowest mean squared error (MSE) of 1.5E-3.

$$\mu_g = \mu_{max}\left(\frac{I}{K_I + I}\right)e^{-\left(\frac{T-T_{opt}}{\theta}\right)^2} \quad (2)$$

The overall expression follows the Arrhenius form where the maximum specific growth rate (μ_{max}) and the light dependency term comprise the pre-exponential factor. For light-dependency, Monod kinetics was assumed, where K_I is the half-light saturation constant ($\mu E/m^2s$). Temperature dependence was modeled as a Gaussian function where T_{opt} represents the mean of the curve or the temperature where the corresponding growth rate is the highest (Franz et al., 2012). Growth rate levels off exponentially as the temperature deviates (either positively or negatively) from T_{opt}. Accordingly, θ is the temperature distribution parameter that is analogous to the standard deviation.

3.3 Modeling death rate

In literature, the death rate was often considered as a constant parameter whose value was determined via parameter estimation (Darehshouri et al., 2008). This method may seem appropriate for this study as the exact cause(s) of cell death during night time has not been confirmed. However, attempts to estimate as a static parameter resulted in poor model fitting where in most cases the value reached the lower bound. In addition, higher rates of cell death were observed on nights 2 and 4.

$$\mu_d = k_D e^{-C_D I} \quad (3)$$

The death rate was modeled empirically which ultimately resulted in an Arrhenius form dependent on light intensity rather than temperature (3). This was due to possible overlap with the expression for μ_g, and to account for possible PCD in the absence of light. Equation (3) introduces two additional fitting parameters: specific death rate k_D and the death constant C_D. Performing parameter estimation with equations (2) and (3) resulted in a good estimation (Fig. 3) that was able to adequately capture the concentration dynamics. The resultant mean squared error was 1.47E-3. The values of the estimated parameters and their lower/upper bounds are summarized in Table 2.

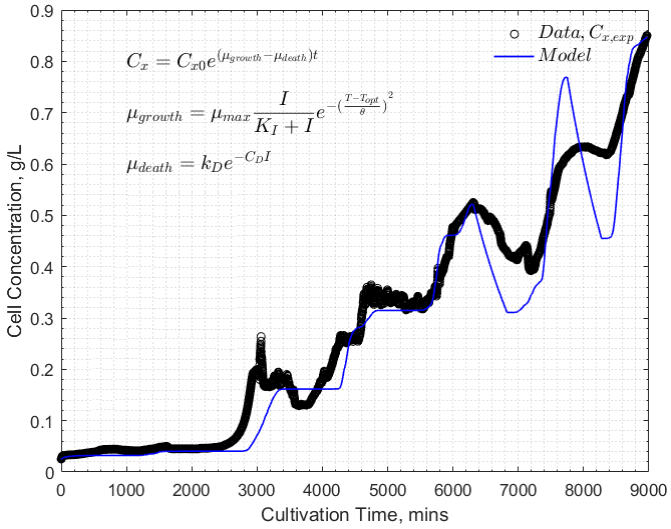

Figure 3 Parameter estimation considering rate expressions for cell growth and death as functions of light intensity and temperature.

Table 2. Values of parameter estimators with bounds

Parameter	Value	Upper Bound	Lower Bound
μ_{max}	0.0035 min^{-1}	0.01	0.0001
K_I	384.5 $\mu E/m^2s$	100	800
T_{opt}	27.9°C	10	50
θ	9.8°C	0.001	100
k_D	0.0011 min^{-1}	0.01	0.0001
C_D	187.6	0.001	Positive

4. DOWNSTREAM MODELING

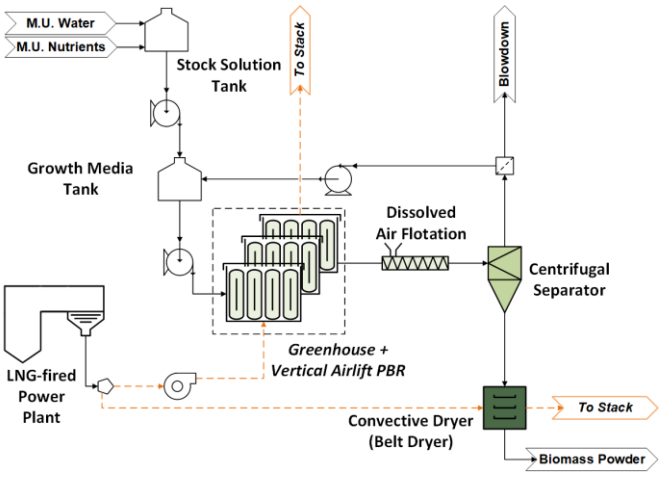

Figure 4 Flow diagram of the algal BPFS process. Yellow lines represent bypass streams.

A simplified flow diagram is shown in Figure 4. For the purpose of constructing mass and energy balances, dissolved air flotation (DAF) and centrifugation was assumed for

harvesting and dewatering, respectively. Centrifugation can achieve biomass concentration up to 25 solid wt% (Fasaei et al., 2018). However, in order for algal powder to be transported and blended, water content needs to be minimized to <10 wt% (Crocker et al., 2018), which requires drying. While traditionally an energy intensive process, the on-site integration with the LNG-fired power plant means that flue gas can be used as a source of cost-free waste heat.

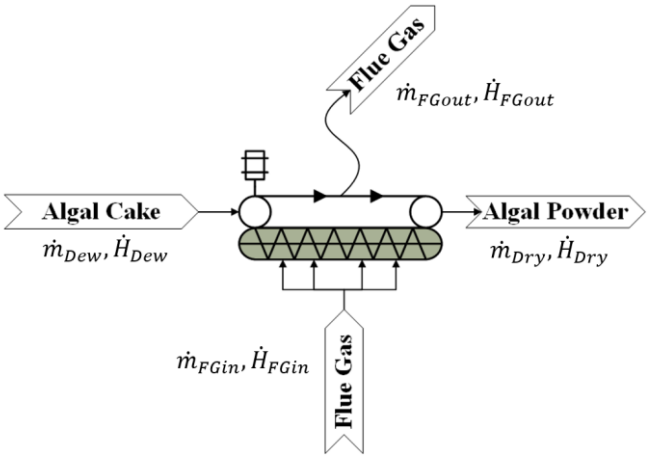

Figure 5. Adiabatic process for convective flue gas drying

Black box models were used for harvesting, dewatering and blowdown purge steps. The biomass recoveries at harvest and dewatering were 91% and 95% respectively (Niaghi et al., 2015, Molina Grima et al., 2003) and energy consumption was scaled using literature values. For the drying process (Fig. 5), the following adiabatic convective dryer model was used (4).

$$\dot{H}_{Dew} + \dot{H}_{FG_{in}} = \dot{H}_{out} + \dot{H}_{FG_{out}} \tag{4}$$

Water removal occurs both from the convective force of air and heat transfer from the flue gas. No external heat is supplied and the blower energy requirements are calculated separately. The enthalpy of the incident flue gas $\dot{H}_{FG_{in}}$ can expressed as the sum of specific heat capacity and the latent heat of humidity:

$$\dot{H}_{FG_{in}} = \left(c_p^{FG} + c_p^{H2O}\xi_{in}\right) \cdot T^{in} + H_{LAT}\xi_{in} \tag{5}$$

Setting $TM = 10\ wt\%$ as the target moisture, the removal rate of water and the required flue gas flowrate can be calculated by the following equations:

$$\dot{Evp} = \dot{m}_{H2O}^{Dew} - \frac{TM * \dot{m}_{Algae}^{Dew}}{1 - TM} \tag{6}$$

$$\dot{m}_{FG} = \frac{\dot{Evp}}{\xi_{in} - \xi_{out}} \tag{7}$$

ξ_{in} and ξ_{out} are the relative humidities of incident and outlet flue gases. The outlet flue gas temperature was set to 55°C according to Giostri et al., implying a temperature drop of 45°C (Giostri et al., 2016). The relative humidities are calculated by equations (8) and (9).

$$\xi_{in} = \frac{MW_{Water}}{MW_{FG}} \cdot \frac{p_{FG_{in}}^{sat} * X_{H2O}}{p_{FG_{in}} - (p_{FG_{in}}^{sat} * X_{H2O})} \tag{8}$$

$$\xi_{out} = \frac{\dot{H}_{FG_{in}} - c_p^{FG} T^{out}}{c_p^{H2O} T^{out} + H_{LAT}} \tag{9}$$

The model has 4 unknowns ($\dot{H}_{FG_{in}}, \dot{m}_{FG}, \xi_{in}, \xi_{out}$) and 4 equations (5, 7, 8, 9). The values of the unknowns and the parameters are summarized in Table 3.

Table 3. Parameters and solved unknowns for the adiabatic dryer

Parameter		Value
$\dot{Evp}$	Water evaporation rate, kg/hr	47.2
TM	Target biomass moisture, wt %	10
H_{LAT}	Latent heat of moisture, kJ/kg	2260
c_p^{FG}	Heat capacity of flue gas, kJ/kgC	1.05
c_p^{H2O}	Heat capacity of water, kJ/kgC	4.19
X_{H2O}	Water content in flue gas, wt%	5
T^{in}	Flue gas inlet temperature, °C	100
T^{out}	Flue gas exit temperature, °C	55

5. SUSTAINABILITY ASSESSMENT

5.1 Performance indicators for sustainability assessment

Prior to sustainability assessment, the pilot plant was up-scaled 1,000 times to remove any scale-dependent effects when measuring performance indicators. The scaled-up process with a PBR volume of 15,000 m^3 was simulated in MATLAB as a semi-batch, wherein cultivation and media preparation were operated as batch and the remaining downstream units were operated as continuous. Economic and environmental sustainability of the *Chlorella vulgaris* BPFS process was measured by with the unit cost of goods manufactured (unit COGM) and carbon footprint per functional unit indicators. Unit COGM measures the total annual cost of production divided by the total amount of produced product (10). Due to the early maturity and small scale of the BPFS plant, Lang factors from Towler and Sinnott (2013) was used to estimate fixed operating expenses such as labor and overhead (Towler and Sinnott, 2013).

$$Unit\ COGM = \frac{OPEX^{Variable} + OPEX^{Fixed} + CAPEX}{\sum_{year} Algal\ Powder\ Production} \tag{10}$$

OPEX and CAPEX represent operating expenses and capital expenses, respectively. Variable operating expenses depend on the plant operation, and include costs of utilities and raw materials. Fixed operating expenses includes labor costs and site maintenance. Cost factors for OPEX were referenced from Clippinger and Davis (2019) (Clippinger and Davis, 2019). Capital expenses include annual payments on plant capital with interest. A capital recovery factor of 6.5% was used assuming an annual discount rate of 5%. Specific carbon footprint (CF) measures the total cradle-to-gate global warming impact of algal BPFS production per functional unit. This includes any indirect greenhouse gas (GHG) emissions from raw material and utility production and consumption. Note that due to the integration with the LNG-fired power plant with flue gas bypass, CO_2 emissions from the PBR off gases were not counted as direct emissions.

$$Specific\ CF = \frac{\sum Direct\ \&\ indirect\ GHG\ emissions}{\sum_{year} Algal\ Powder\ Production} \quad (11)$$

For the purpose of assessment, the functional unit was set to "1 ton of algal powder (A.P.) with <10 wt% moisture"

5.2 Baseline assessment results

The baseline values for the measured indicators were 2768 USD/ton A.P. and 1.3 ton CO_2-eq/ton A.P. from a mean biomass productivity of 0.13 kg/m^3/day. The breakdown graphs for constituent cost and emission components are displayed in Figure 6.

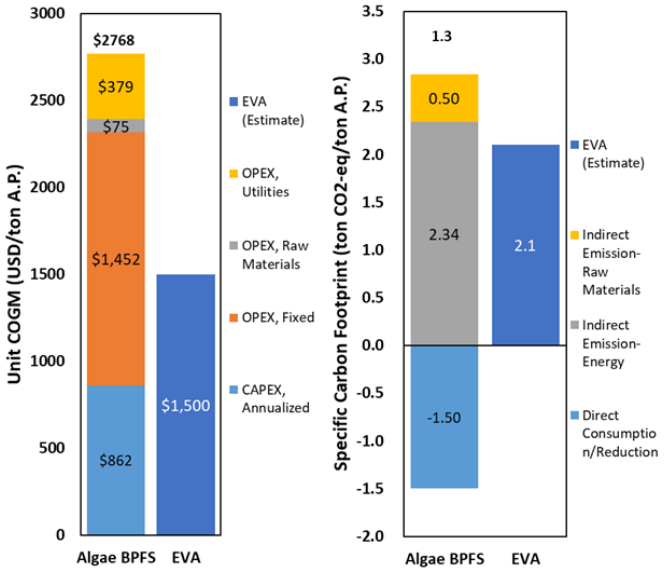

Figure 6. Breakdown of the unit COGM and specific carbon footprint for algal BPFS production

The high cost of production is primarily attributed to the cost of the greenhouse and PBRs. Of the 1452 USD/ton fixed operating costs, labor and maintenance account for 699 USD/ton and 629 USD/ton respectively. In the case of carbon footprint, a nominal reduction is achieved when the algal BPFS is compared with the conventional EVA resin. The majority of emissions were indirect in the form of electricity production. Large amounts of electricity were consumed by flue gas blowers operating 24 hours a day, and at a pressure drop of 0.12 bar. Due to the trade-off relationship of higher unit COGM versus saved GHG emissions, the cost of CO_2 avoided can be calculated as follows (12)

$$Cost_{Avoided} = \frac{COGM_{Algae\ BPFS} - COGM_{EVA}}{CF_{EVA} - CF_{Algae\ BPFS}} \quad (10)$$

At baseline conditions, the cost of CO_2 avoided for the algae BPFS plant was 1509 USD/ton CO_2.

5.3 Predicting seasonal biomass production with uncertainty

The growth model was used to predict seasonal average biomass productivities and estimate how plant economics and environmental emissions change with climate conditions. Climate data from the Korea Meteorological Administration was appropriated to greenhouse conditions using pilot plant data as reference. Random 149 hour intervals were sampled between December – February, March – May, June – August, and September – November corresponding to Spring, Summer, Fall, and Winter seasons, respectively. For each sampled interval, biomass growth was predicted with the current model and sustainability assessment was performed for the up-scaled scenario. For each season, Monte Carlo sampling of 149 hour intervals was performed 1,000 times. Figure 7 displays the average values of performance indicators for each season, with error bars representing one standard deviation from the empirical distribution.

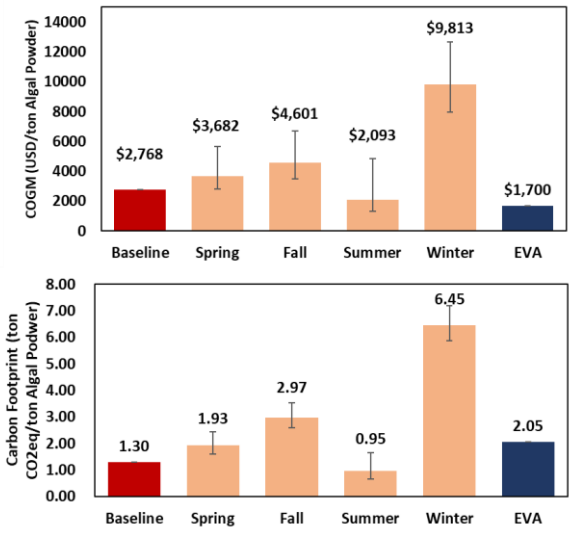

Figure 7. Predicted seasonal average estimates for performance indicators using Monte Carlo simulation of meteorological data.

Figure 7 verifies that the performance of the algal BPFS plant is highly dependent on natural light and temperature variabilities. Korea has distinct seasonal weathers with warm and dry spring/fall, hot and humid summers, and cold and dry winters. A larger error bar was observed for the Summer due to Korea's monsoon season, in which periods of sporadic rainfall result in reduced photosynthetically available radiation (PAR). Both economics and environmental sustainability falls dramatically during the winter season. This was due to lower predicted biomass productivities despite unchanging expenses incurred during plant operation. The average biomass productivity during December – February was 0.0072 kg/m^3/day.

6. DISCUSSION

Validating the growth model should take precedence before any meaningful R&D decisions are made. In this study, a single dataset from the cultivation pilot plant was used to perform parameter estimation. In addition, for appropriating ambient light intensity and temperature data to the greenhouse a simple scaling factor was used. The accuracy and scope of the prediction model could benefit from additional experimental datasets conducted over a wider range of climate conditions. Measurements of PAR and culture temperature inside the greenhouse alone, can enable a more rigorous appropriation model taking into consideration effects such as sunlight albedo.

With the present results, it is difficult to guarantee the sustainability of algal BPFS despite significant improvements over previous biofuel applications. Disregarding natural variabilities, the greatest hurdles to sustainability seem to be the high upstream capital costs at the cultivator and high energy consumption from flue gas aeration. Regarding the latter, testing a range of flue gas aeration speeds and its effect on settling and biomass productivity can enable a PBR mass transfer model to supplement growth kinetics. Optimal aeration speeds can subsequently be determined through optimization.

A limitation of this study was that the uncertainty of parameter estimators was not considered, focusing only on the effect of natural variabilities. The effect of both model uncertainties and natural variabilities can be quantified simultaneously with second-order Monte Carlo simulations (Wu and Tsang, 2004). This would allow a more complete assessment of risk when assessing the viability for further scale-up.

REFERENCES

Béchet, Q., Shilton, A. & Guieysse, B. (2013). Modeling the effects of light and temperature on algae growth: State of the art and critical assessment for productivity prediction during outdoor cultivation. *Biotechnology Advances,* 31**,** 1648-1663.

Clippinger, J. & Davis, R. E. (2019). Techno-economic analysis for the production of algal biomass via closed photobioreactors: future cost potential evaluated across a range of cultivation system designs. *In:* (NREL), N. R. E. L. (ed.). Golden, CO (United States).

Crocker, M., Groppo, J., Kesner, S., Mohler, D., Pace, R., Santillan-Jimenez, E., Wilson, M., Schambach, J., Stewart, J. & Zeller, A. (2018). A Microalgae-Based Platform for the Beneficial Re-use of Carbon Dioxide Emissions from Power Plants. United States.

Crocker, M., Zeller, A., Quinn, J. C., Quiroz Nuila, D., Beckstrom, B., Kesner, S., Mohler, D., Pace, R. & Wilson, M. (2020). CO2 to Bioplastics: Beneficial Re-use of Carbon Emissions from Coal-fired Power Plants using Microalgae. United States.

Darehshouri, A., Affenzeller, M. & Lütz-Meindl, U. (2008). Cell death upon H(2)O(2) induction in the unicellular green alga Micrasterias. *Plant biology (Stuttgart, Germany),* 10**,** 732-745.

Demirbas, A. & Fatih Demirbas, M. (2011). Importance of algae oil as a source of biodiesel. *Energy Conversion and Management,* 52**,** 163-170.

Fasaei, F., Bitter, J. H., Slegers, P. M. & van Boxtel, A. J. B. (2018). Techno-economic evaluation of microalgae harvesting and dewatering systems. *Algal Research,* 31**,** 347-362.

Franz, A., Lehr, F., Posten, C. & Schaub, G. (2012). Modeling microalgae cultivation productivities in different geographic locations – estimation method for idealized photobioreactors. *Biotechnology Journal,* 7**,** 546-557.

Gerber, L. N., Tester, J. W., Beal, C. M., Huntley, M. E. & Sills, D. L. (2016). Target Cultivation and Financing Parameters for Sustainable Production of Fuel and Feed from Microalgae. *Environmental Science & Technology,* 50**,** 3333-3341.

Giostri, A., Binotti, M. & Macchi, E. (2016). Microalgae cofiring in coal power plants: Innovative system layout and energy analysis. *Renewable Energy,* 95**,** 449-464.

Guest, J. S., van Loosdrecht, M. C. M., Skerlos, S. J. & Love, N. G. (2013). Lumped Pathway Metabolic Model of Organic Carbon Accumulation and Mobilization by the Alga Chlamydomonas reinhardtii. *Environmental Science & Technology,* 47**,** 3258-3267.

Lee, E., Jalalizadeh, M. & Zhang, Q. (2015). Growth kinetic models for microalgae cultivation: A review. *Algal Research,* 12**,** 497-512.

Li, X., Wang, X., Duan, C., Yi, S., Gao, Z., Xiao, C., Agathos, S. N., Wang, G. & Li, J. (2020). Biotechnological production of astaxanthin from the microalga Haematococcus pluvialis. *Biotechnology Advances,* 43**,** 107602.

Molina Grima, E., Belarbi, E. H., Acién Fernández, F. G., Robles Medina, A. & Chisti, Y. (2003). Recovery of microalgal biomass and metabolites: process options and economics. *Biotechnology Advances,* 20**,** 491-515.

Niaghi, M., Mahdavi, M. A. & Gheshlaghi, R. (2015). Optimization of dissolved air flotation technique in harvesting microalgae from treated wastewater without flocculants addition. *Journal of Renewable and Sustainable Energy,* 7**,** 013130.

Razon, L. F. & Tan, R. R. (2011). Net energy analysis of the production of biodiesel and biogas from the microalgae: Haematococcus pluvialis and Nannochloropsis. *Applied Energy,* 88**,** 3507-3514.

Scholes, C. A., Ho, M. T. & Wiley, D. E. (2016). Membrane-Cryogenic Post-Combustion Carbon Capture of Flue Gases from NGCC. 4**,** 14.

Towler, G. & Sinnott, R. (2013). Chapter 7 - Capital Cost Estimating. *In:* TOWLER, G. & SINNOTT, R. (eds.) *Chemical Engineering Design (Second Edition).* Boston: Butterworth-Heinemann.

Zeller, M. A., Hunt, R., Jones, A. & Sharma, S. (2013). Bioplastics and their thermoplastic blends from Spirulina and Chlorella microalgae. *Journal of Applied Polymer Science,* 130**,** 3263-3275.